Structural and optical properties of DC sputtered $Al_xO_y/Cr/Al_xO_y$ multilayer selective absorber coatings

Justine J. Tibaijuka [a,*], Justine S. Nyarige [b], Mmantsae Diale [b], Nuru R. Mlyuka [a], Margaret E. Samiji [a]

[a] University of Dar es Salaam, Department of Physics, P.O. Box 35063, Uvumbuzi Road, Dar es Salaam, Tanzania
[b] University of Pretoria, Department of Physics, Private Bag X20, Hatfield, 0028, South Africa

ARTICLE INFO

Keywords:
Sputtering
Multilayered selective absorbers
Alumina
Chromium

ABSTRACT

$Al_xO_y/Cr/Al_xO_y$ multilayered selective absorber was theoretically optimized using the individual layers' optical constants acquired through fitting the transmittance and reflectance measurements into SCOUT software. The optimized multilayer was deposited onto polished aluminium substrates by DC magnetron sputtering at room temperature. The structural analysis of the multilayer stack revealed low crystalline diffraction peaks of Cr at $2\theta \approx 43.3^\circ$ ascribed to (110) diffraction plane of BCC Cr metal. However, due to the amorphous nature of the deposited films, no Al_xO_y phase was detected by XRD. SEM and AFM analysis revealed the uniformly and densely distributed small grains with a considerably average surface roughness of ~5.6 nm. The deposited $Al_xO_y/Cr/Al_xO_y$ multilayered stack was found to have an optical absorptance of 0.91 and thermal emittance of 0.12 at a temperature of 373 K, which is potential and suitable for selective solar absorbers applications.

1. Introduction

Solar thermal conversion through concentrating solar power (CSP) systems is among the fast-growing technologies as the alternative way to minimize the dependence on fossil fuels [1,2]. To convert solar radiation into heat energy, one requires an efficient selective solar absorber that can withstand high-temperature operation while maintaining selectivity. Ideally, selective solar absorbers should absorb much in the solar UV–Vis–NIR spectrum region and emit none/low in the infrared region extending above 2500 nm [3,4]. So far, no single material has been reported to meet these requirements and operate well at high operation temperatures beyond 400 °C. To address this, several absorber designs, such as semiconductor metal tandems [2], metal-dielectric composites [5–7] and multilayer absorbers [l, 8], to mention a few, have been researched and developed for wider solar-thermal applications. Recently, the multilayer interference stack design, among others, has been attracting the competing interest of researchers. Among the multilayer interference stacks, the typical multilayer absorbers consisting of a semitransparent metal layer sandwiched between the dielectrics (i.e. Dielectric/Metal/Dielectric, DMD) are promising due to their feasible spectral properties over a wide range of solar spectrum and wide incident angles, low thermal emittance, low cost and the flexibility of production, which are potential for medium and high-temperature applications [9–11]. The spectral selectivity in DMD multilayer absorbers is enhanced by multiple reflections and interferences of incident radiation and the Surface Plasmon Polaritons (SPP) confined along the dielectric-metal interface [12,13].

So far, the multilayer-based selective solar absorbers coatings for solar thermal conversions such as $Cr_xO_y/Cr/Cr_2O_3$ [14], $HfO_2/Mo/HfO_2$ [15], MgO/Zr/MgO [16,17], $Al_xO_y/Al/Al_xO_y$ [18], $Al_xO_y/Ni/Al_xO_y$ [10], $Al_2O_3/Mo/Al_2O_3$ [19], $Al_2O_3/Pt/Al_2O_3$ [3], $Cr_2O_3/Cr/Cr_2O_3$ [20, 21], $ZrO_x/Zr/ZrO_x/Al_xO_y$ [22] have been fabricated by different methods such as chemical vapour deposition, pulse laser deposition, spray pyrolysis, sol-gel spin coating [23], thermal evaporation [3,22] and sputtering [2,5,7,14]. However, the selectivity for most of such coatings are still technically challenged by factors such as inter-diffusion, oxidation, high humidity, corrosion, and poor interlayer adhesion, arising when the device is operated at temperatures beyond 400 °C and in the air [13,22,24]. In this regard, there has been an increase in the search for new transition metals and microstructure modification through modelling, optimization of material characteristics and preparation techniques to suppress the fore mention constraints [12].

Explicitly, the multilayer $Al_xO_y/Cr/Al_xO_y$ is a potential candidate

* Corresponding author.
E-mail addresses: jtibaijuka14@gmail.com, justine.tibaijuka@udsm.ac.tz (J.J. Tibaijuka).

that has not been fully explored for selective solar absorber coating. The potential is geared by its environmentally friendly components with excellent properties for fabricating spectrally selective solar absorbers such as high melting point, low thermal conductivity, corrosion-free, good oxidation resistance and intrinsic selectivity [3,12,21,25]. Furthermore, besides having full spectral transparency from ultra-violet to mid-infrared, wide band gap and tunable refractive index, the alumina dielectric component has proved its suitability as a diffusion barrier [26,27]. The latter makes alumina dielectric the first choice to prevent inter-diffusion among the interlayer stacks of multilayer-based selective absorbers. Likewise, Cr metal, besides being an intrinsic selective absorber, has also demonstrated its suitability as DMD selective absorber using other dielectrics such as Cr_2O_3 [14,21]. Thus, combining Cr metal with excellent alumina dielectric is potentially ideal for efficient and thermally stable selective solar absorber coatings.

Additionally, several studies have revealed that the optical properties and thermal stability of the DMD selective coatings rely on deposition techniques and conditions [8,16,21]. Among these methods, sputtering is versatile and suitable for large-area deposition due to its relatively high deposition rate and being environment-friendly. Furthermore, most thin films produced by this method have high-quality uniform films with exceptional physical and optical properties [28]. Such potentials however, are still unrealized on the properties of $Al_xO_y/Cr/Al_xO_y$ selective solar absorbers. Therefore, this study systematically reports for the first time the structural and optical characteristics of DC sputtered $Al_xO_y/Cr/Al_xO_y$ multilayer selective solar absorbers coated on high-shining Al substrates.

2. Materials and methods

2.1. Sample preparation

All films (Cr, AlxOy, and $Al_xO_y/Cr/Al_xO_y$) were deposited onto Soda Lime Glass (SLG) and Al substrates at room temperature using the BALZERS BAE 250 coating unit. Before deposition, the sputtering chamber was evacuated to a minimum pressure of 10^{-6} mbar using a built-in turbo-molecular pump backed up with a rotary vane pump. Similarly, the glass and Al substrates were intensively cleaned to remove the grease and other embedded impurities as ascribed in Tibaijuka et al., [29]. In all cases, the SLG was chosen to optimize the thickness, optical transmittance, and reflectance of film coating, whereas Al substrate was selected to ascertain the optical performance of the multilayer stack.

The top and bottom Al_xO_y layers were reactively sputtered at a power of 200 W and Oxygen flow rate of 4.15 SCCM from high purity Al target (99.99%) commercially acquired from Plasmaterials Inc. Prior to deposition, the Al target was pre-sputtered for 10 min to remove the target's surface contaminants. Also, to minimize arcing, the sputtering gas was first introduced in the chamber and allowed to stabilize for 5 min, and thereafter, the reactive oxygen gas was introduced and increased slowly to the desired value. Likewise, the Cr films were deposited at the power of 25 W and Argon flow rate of 15 SCCM from high purity Cr target (99.99%) commercially acquired from Plasmaterials Inc. as ascribed elsewhere in Tibaijuka et al., [28]. In all depositions, the working pressure of a chamber was fixed at 5×10^{-3} mbar.

Before depositing the multilayer, the optimal individual layer thicknesses suitable for selectivity were determined from the simulated $Al_xO_y/Cr/Al_xO_y$ multilayer absorber. The multilayer stack was simulated using the optical constants of the substrates and individual layers, determined by fitting the measured transmittance and reflectance spectra into SCOUT software 2.4 [30] with the proper dielectric functions describing their optical behaviours. For the glass substrate, the optical constants were extracted from the SCOUT database using the "microscope slide, Vis" model, while that of the Al substrate was modelled using the dielectric function built with dielectric background, Drude model and a harmonic oscillator [2,21,30]. The chromium mid-layer was modelled using dielectric functions consisting of the complex dielectric background and Brendel-Bormann oscillators, while the dielectric Al_xO_y was modelled using the dielectric function comprising dielectric background and harmonic oscillators [2,21,30].

2.2. Characterization of samples

The film thicknesses were determined by measuring the step produced by a Teflon tape laid on a substrate before deposition, using the Alpha Step surface profiler. The film's structural phases were determined by Bruker D2-Phaser X-ray Diffractometer (XRD) that was operated at a scanning rate of 0.050 per minute for the 2θ ranging from 20° to 70° using a 0.1504 nm wavelength Cu K-α radiation. The obtained phases were analyzed using reference PDF data in the ICDD database. The sample structures were further analyzed with the help of Raman spectroscopy by employing Raman laser excitation with 532 nm wavelengths. The surface morphology and topology of the coating were examined using Field Emission-Scanning Electron Microscopy (FE-SEM) (Zeiss Crossbeam 540 model) and Nanoscope IIIA atomic force microscope (AFM). The AFM and SEM images were respectively analyzed for grains' size and surface roughness using WSxM software (version 4.0) and ImageJ 2 software as ascribed in Ref. [31]. Using a double beam PerkinElmer Lambda 1050+ UV–Vis–NIR spectrophotometer with a 5-nm scan interval, the optical transmittance and reflectance of the films in the wavelength range of 250–2500 nm were measured. The reflectance in the infrared band up to 15,000 nm was characterized using Fourier transform infrared (FT-IR) spectroscopy. The spectral solar absorptance (α) and thermal emittance (ε) were computed from the measured reflectance using equations (1) and (2).

3. Results and discussion

3.1. Structure and morphology of the films

3.1.1. XRD and Raman analysis

Fig. 1a depicts the XRD pattern of a typical $Al_xO_y/Cr/Al_xO_y$ deposited on an SLG substrate at room temperature. The XRD pattern reveals the diffuse and low-intensity broad peaks due to their amorphous nature. The prominent broad peak was observed at $2\theta \approx 43.3°$ which can be associated with the (110) plane of BBC Cr films as per Joint Committee of Powder Diffraction Standards (JCPDS) (PDF#06–0694). No distinct crystallinity peaks associated with Al_xO_y were observed due to the amorphous nature of the films as alumina films are said to crystallizes at higher temperatures ~900 °C [3,22]. However, the analysis performed on the sample using Raman spectroscopy (Fig. 1b) revealed a broad peak at ~500-700 cm^{-1}, which was ascribed to Al–O vibration modes [32].

Fig. 2 shows the quantitative analysis of the substrate and the deposited coatings using EDX spectra. As seen from Fig. 2a, only one peak ascribed to Al was observed, which confirms the purity of the used substrate. The EDS spectra in Fig. 2b revealed the presence of the principal elements (Aluminium, Oxygen and Cr) and other elements, such as Calcium, Silicon, and carbon arising from the glass substrate and carbon coating done before measurements. The Cr, Al and O peaks were found at energies of 14.0 keV, 1.5 keV and 0.52 keV, respectively, which is consistent with EDX results of amorphous Chromium and Alumina films reported in other literature. Besides, the EDX analysis revealed further that the as-deposited Al_xO_y films were nonstoichiometric.

3.1.2. SEM and AFM analysis

Fig. 3 presents the SEM micrograph of the deposited $Al_xO_y/Cr/Al_xO_y$ multilayered solar absorber coating onto the Al substrate. The SEM micrographs reveal a uniform surface with some clustered grains, which could be due to high deposition power and Argon flow rate on depositing the top Al_xO_y layer. Furthermore, Fig. 3b-inset revealed the columnar growth structure on both the bottom and top dielectric layer; however,

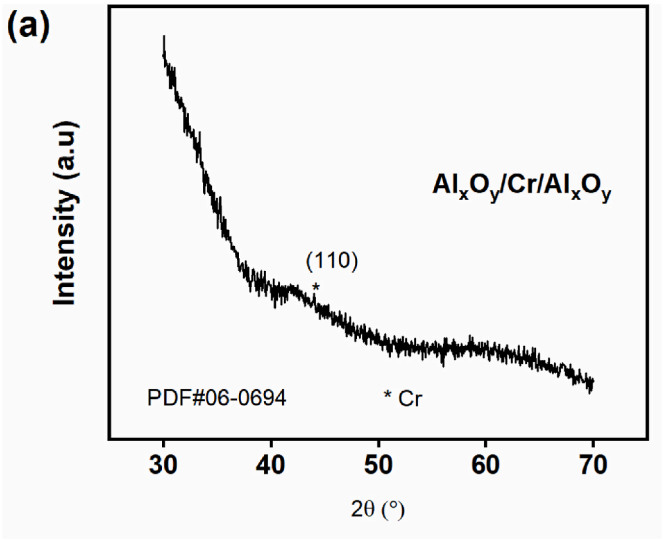

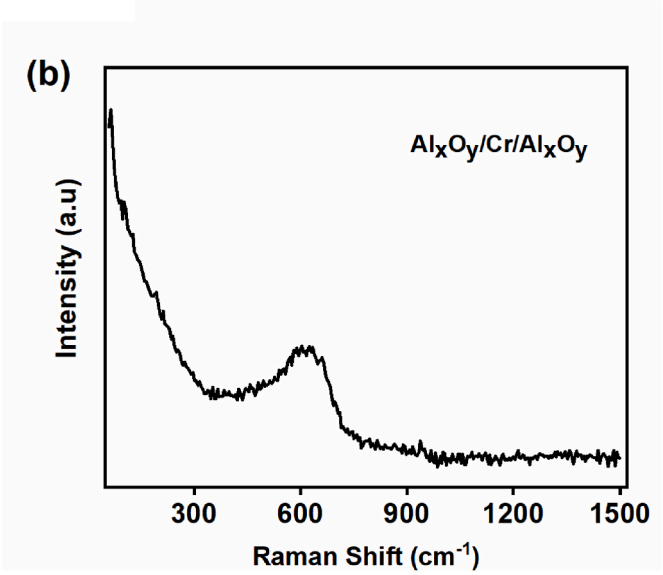

Fig. 1. XRD (a) and Raman (b) pattern of deposited $Al_xO_y/Cr/Al_xO_y$ multilayer stack selective solar absorber on SLG substrate.

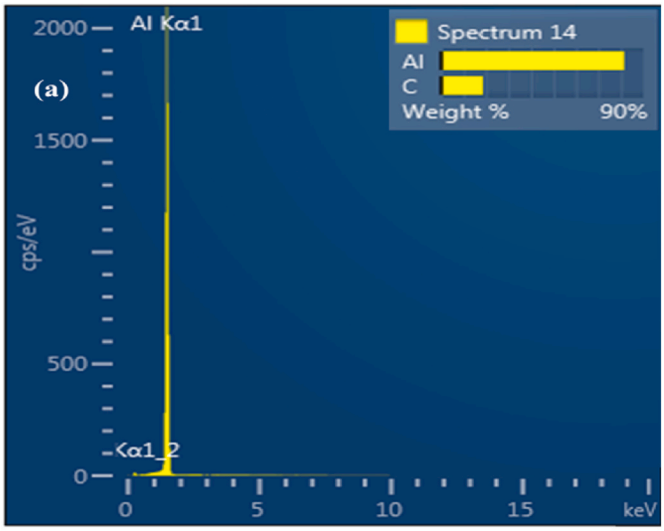

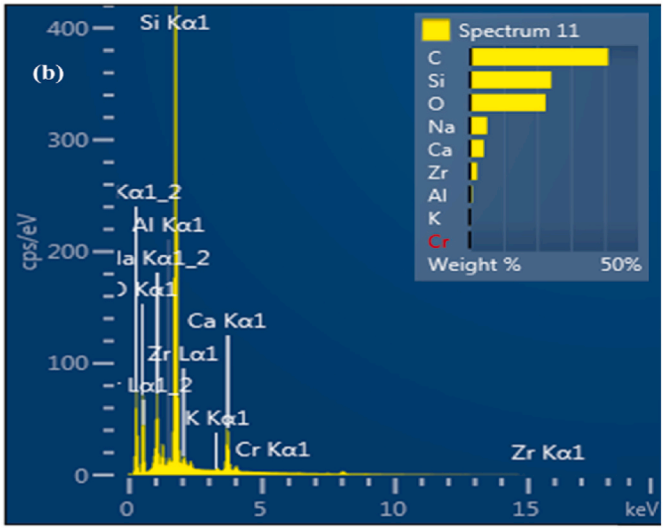

Fig. 2. EDX spectra of the substrate (a) and the deposited $Al_xO_y/Cr/Al_xO_y$ multilayered stack selective solar absorber (b).

no columnar growth is seen on the mid layer as its thickness is very thin compared to the rest layers of the coating.

Fig. 4 presents 2D and 3D AFM topographical images of the $Al_xO_y/Cr/Al_xO_y$ multilayered coating deposited onto the SLG substrate. AFM images reveal the small cluster of grains with root-mean-square roughness and average surface roughness (Ra) of ~6.8 nm and ~5.6 nm, respectively. The observed surface roughness is comparable to previously reported roughness for Al_xO_y-based multilayered selective absorbers [1,33]. The average surface height was found to be 20 nm. To analyze the symmetry and sharpness (or peakedness) of the surface height distribution, the skewness and kurtosis values were extracted from the surface height distribution histograms (Fig. 2c) using the WSxM software as ascribed by Tibaijuka et al. [34]. The skewness values of 0.1 and the kurtosis value of 2.7 were recorded, implying that the film's average surface height distribution was dominated by narrower and sharper peaks than valleys [28]. Similarly, the AFM images showed evenly dispersed columnar-like structures on the multilayer's surface, as was in SEM images. As reported in the literature, the columnar structures enhance the coating's capacity to trap the incident light and hence the improved selectivity. Besides, the columnar formations in the selective solar absorber coating have also been documented by other literature [16,35,36].

4. Optical properties

Fig. 5 presents the fitted and experimental optical reflectance of the polished Al substrate used for depositing a multilayer stack. As seen in Fig. 5, the optical reflectance is above 90%, which is suitable for depositing selective solar absorbers. Figs. 6–9 show the optical properties of the deposited individual layers and the multilayer selective absorbers, whose thickness was ~60/10/118 nm for the bottom, mid, and top layers, respectively. As seen in Fig. 6a, both the top and bottom Al_xO_y layers exhibited an average optical transmittance above 70% with an increasing trend towards longer wavelengths. On the other hand, their respective reflectance (Fig. 6b) showed a decreasing trend with the increase of wavelengths. For Cr mid layer (Fig. 8 a,b), the optical transmittance of ~25% and reflectance ~of 45% were recorded, which is suitable for solar thermal applications [20,28].

Figs. 7 and 8c illustrate the refractive indices (n) and extinction

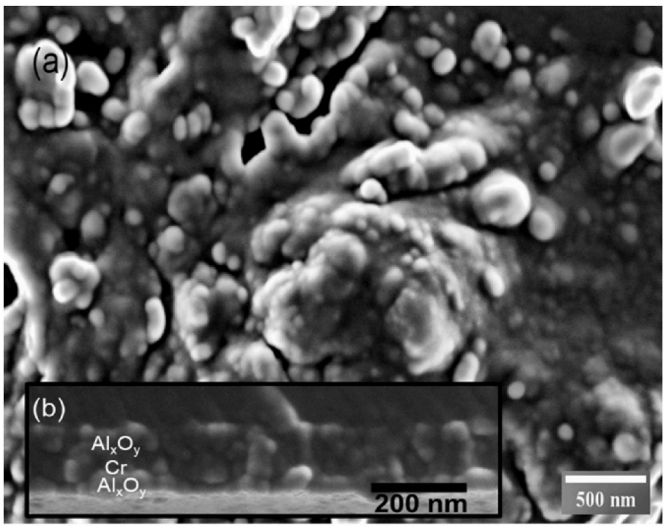

Fig. 3. FE-SEM micrographs of the multilayered $Al_xO_y/Cr/Al_xO_y$ stack optimized on SLG substrate (a) Surface view, inset (b) - cross-sectional view.

coefficients (k) of the deposited bottom Al_xO_y, mid-layer Cr, and the top layer Al_xO_y, respectively extracted through fitting of experimental data obtained by UV–Vis–NIR spectrophotometer and the theoretical model into SCOUT. As seen in Fig. 7, the values of n decreased spontaneously with an increase in wavelength, and small k values close to zero were recorded for both the bottom and top Al_xO_y layers, which signify the dielectric behaviour of the deposited films. This results trend agrees with other authors' reports on alumina films [20,28,34]. Besides, the values of n and k of the middle Cr film (Fig. 8c) demonstrated an increasing trend towards the longer wavelengths, which confirms the characteristic behaviour of metallic chromium film [3,28,34]. It is worth mentioning that, in DMD selective absorber, the layers are chosen in such a way that the metal volume fraction and the refractive index of each layer generally decrease from the substrate to the surface in favour of the absorptance [12].

Fig. 9 shows the reflectance curve and the corresponding schematic diagram of the $Al_xO_y/Cr/Al_yO_x$ multilayer spectral selective absorber. It can be seen that both the measured spectra and simulated curves show good agreement confirming the reliability of the results from the simulations and the experiment. The sample revealed a minimal reflectance in the visible and near-infrared range, 300–1700 nm, which then increased exponentially towards the longer wavelength. The observed low reflectance and the step transition increases of the reflectance curve signify the coating's significant absorption property and spectral selectivity in that region [3]. In most cases, the ratio of solar absorptance (α) to thermal emittance (ε) is often used to ascribe the coatings' optical performance, typically called spectral selectivity. In this study, equation (1) was used to calculate the solar absorptance, which is the percentage of incident light absorbed in the solar spectral range [12].

$$\alpha(\theta) = \frac{\int_{\lambda_1}^{\lambda_c} [1-\rho(\lambda)]G(\lambda)d\lambda}{\int_{\lambda_1}^{\lambda_C} G(\lambda)d\lambda} \tag{1}$$

where θ,$\rho(\lambda)$, λ_1, λ_c and $G(\lambda)$ stand for an incident angle of light, reflectance, minimum wavelength, maximum cutoff solar wavelengths and weight by solar irradiation at AM1.5, respectively. Meanwhile, the thermal emittance (ε) describes the ratio of the object emitted radiation at a specific temperature to the perfect blackbody emitted radiation at the same temperature. In this work, the surface thermal emittance (ε) was computed as the weighted fraction between emitted radiation and the Planck black body distribution at 373 K, using the spectral reflectance and the spectral blackbody emissive power as per equation (2), adapted from Dan et al. [12].

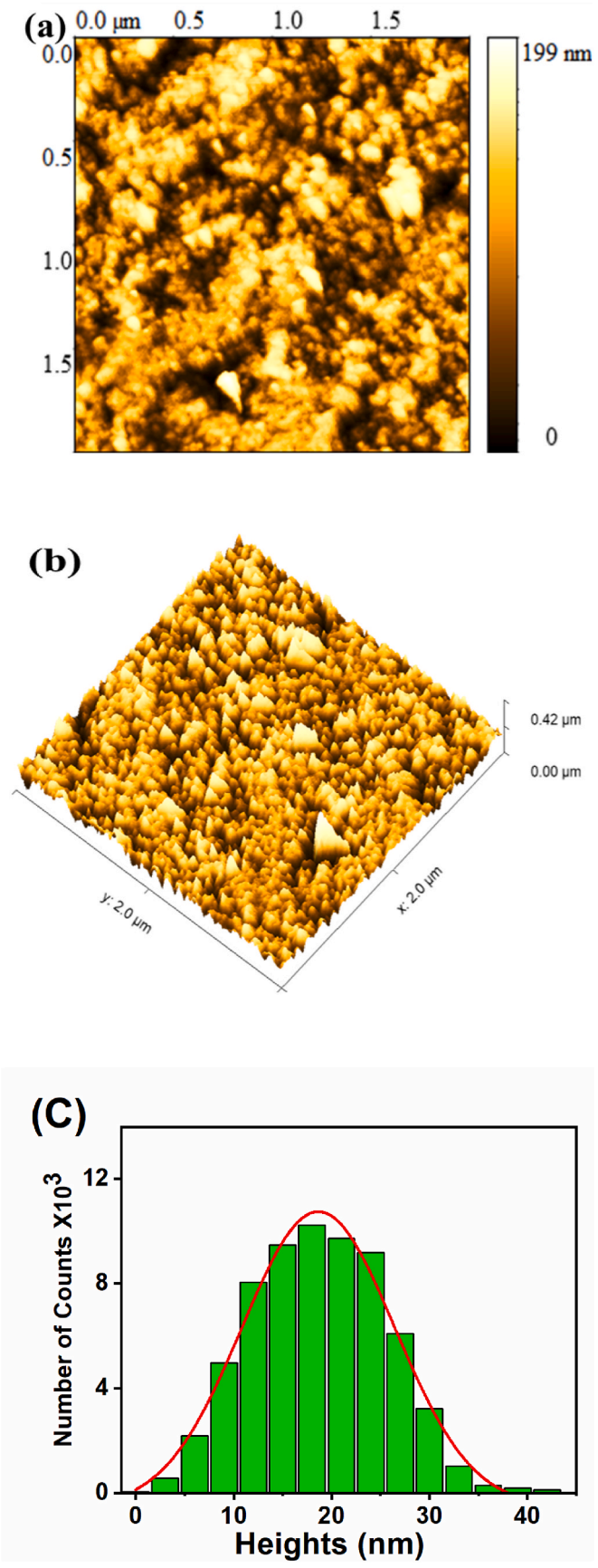

Fig. 4. 2D and 3D AFM images of the $Al_xO_y/Cr/Al_xO_y$ deposited on SLG substrate with their corresponding surface height distribution.

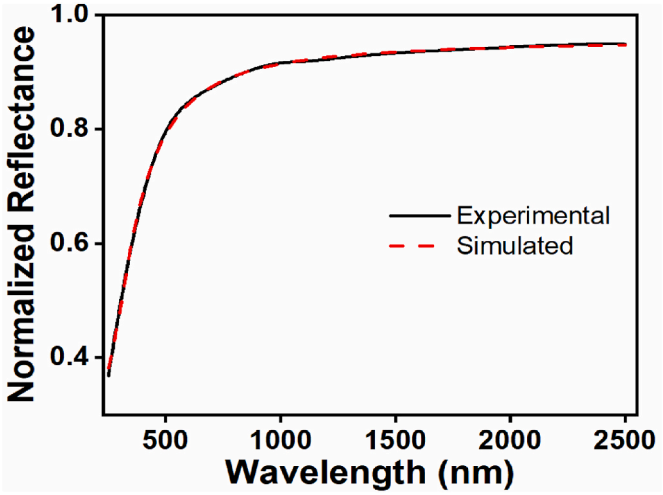

Fig. 5. Simulated and experimental reflectance curves of polished aluminium substrates used for the deposition of the multilayer stack.

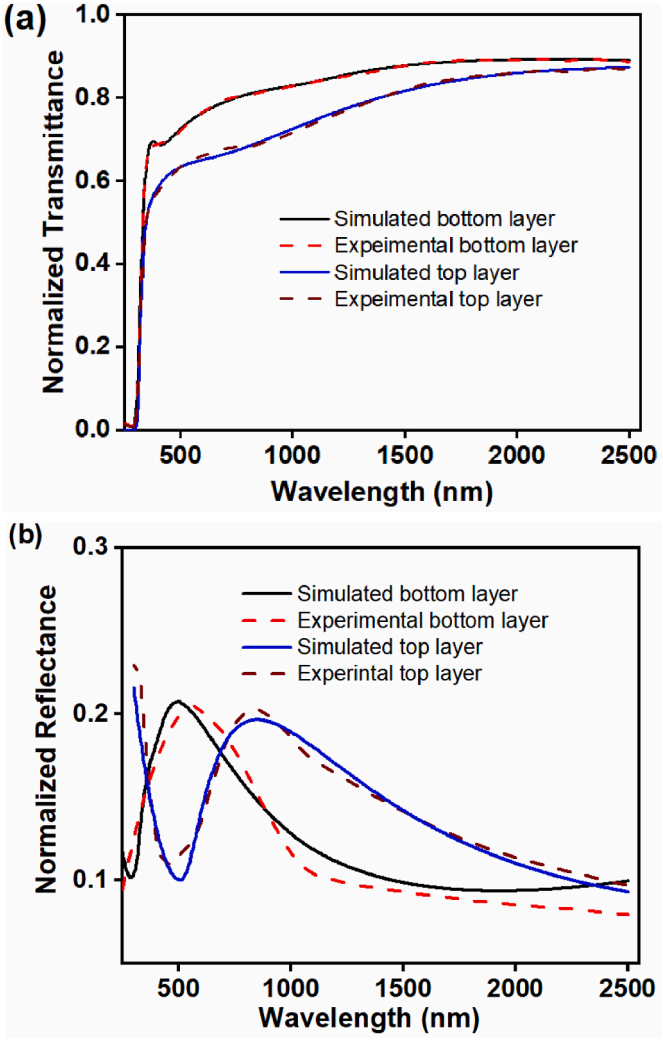

Fig. 6. Experimental and simulated spectra of bottom and top Al_xO_y dielectric layers (a) transmittance curves (b) reflectance curves.

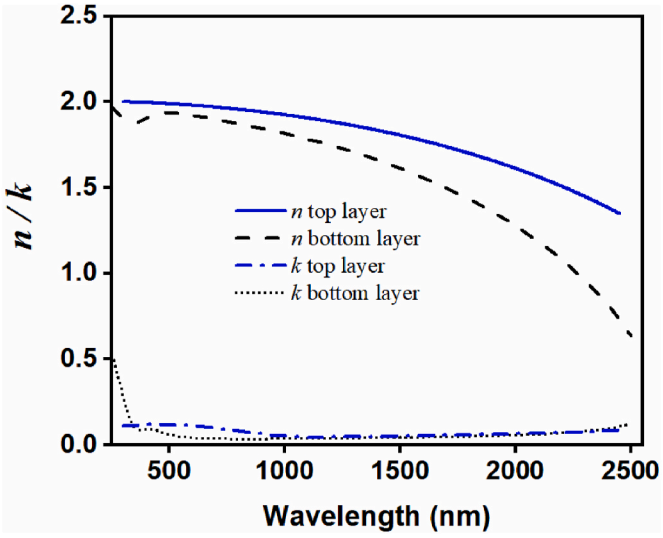

Fig. 7. Optical constants of the top and bottom Al_xO_y dielectric layer used for deposition of the selective coating.

$$\varepsilon(T) = \frac{\int_{\lambda_l}^{\lambda_c} [1-\rho(\lambda)] E_b(\lambda) d\lambda}{\int_{\lambda_l}^{\lambda_c} E_b(\lambda) d\lambda} \quad (2)$$

where $E_b(\lambda)$ represents Plank's black body radiation spectrum. The solar absorptance was found to be 91.4% which is potential and suitable for solar thermal conversions. Moreover, deposited coating recorded the thermal emittance, ε, of ~12% at 373 K, which is recommended for solar thermal conversion applications. These results suggest that the deposited $Al_xO_y/Cr/Al_xO_y$ selective solar absorber coating is potential for low and mid-solar thermal applications. Evaluation of the potential of a multilayer selective absorber also requires consideration of long-term thermal stability and deep cycle studies. For these reasons, this study advises comprehensive analyses of these in future studies.

5. Conclusions

In this work, the multilayered $Al_xO_y/Cr/Al_xO_y$ selective absorber was successfully deposited onto Al substrate using DC magnetron sputtering. The deposition was done at room temperature as the amorphous films are compact and thus can serve to prevent the interfusion between the layers. The structural measurements of the deposited $Al_xO_y/Cr/Al_xO_y$ multilayer stack revealed low crystalline diffraction peaks of Cr at $2\theta \approx 43.3^\circ$ attributed to (110) diffraction plane of BBC Cr metal. No XRD diffraction peaks were observed for Al_xO_y; however, the Raman and EDX measurements depicted the presence of Al and O in the samples. In addition, the deposited sample recorded a solar absorptance α of ~91.4% and thermal emittance ε of ~12% at 373 K, which are potential and recommendable for selective solar absorber applications. These results are promising and indicate the potential of this type of coating for solar selective absorber applications at high temperatures.

Credit authors statement

All authors, with the exception of JS Nyarige, contributed to the study conceptualization. JJ Tibaijuka handled all the sample preparation, data collection and analysis. JS Nyarige was involved in SEM, Raman and XRD characterization. NR Mlyuka, M Diale and ME Samiji handled all financial acquisition and the supervision of work. JJ Tibaijuka wrote the initial manuscripts draft, while all of the other authors reviewed and corrected previous draft. The final manuscript was read and approved by all writers.

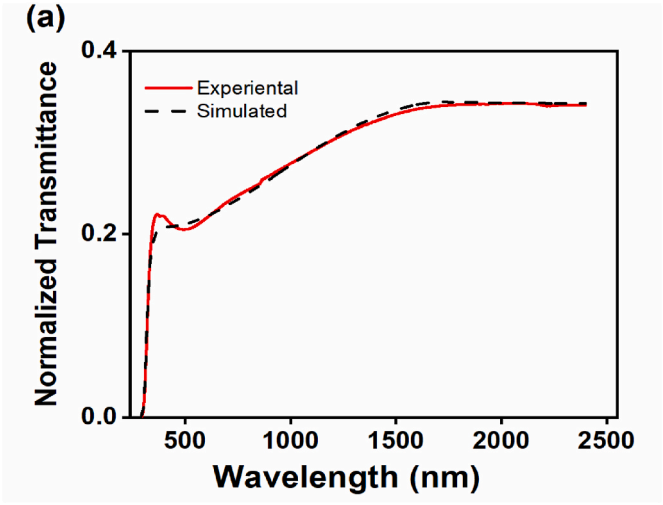

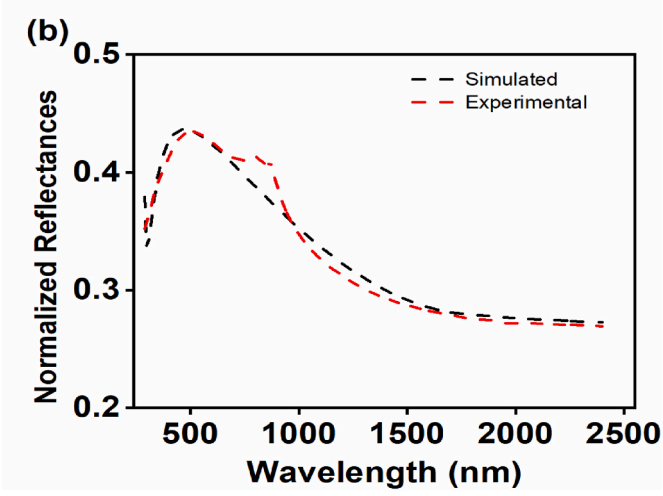

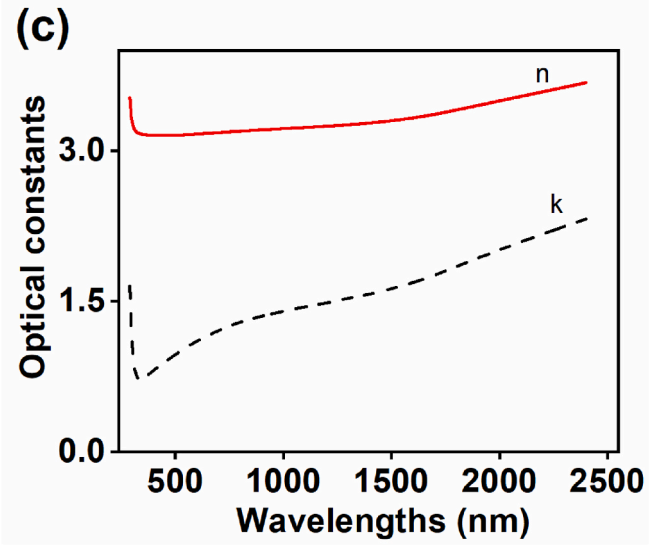

Fig. 8. Experimental and simulated transmittance (a) and reflectance (b) curves and optical constants (c) of Cr mid-layer.

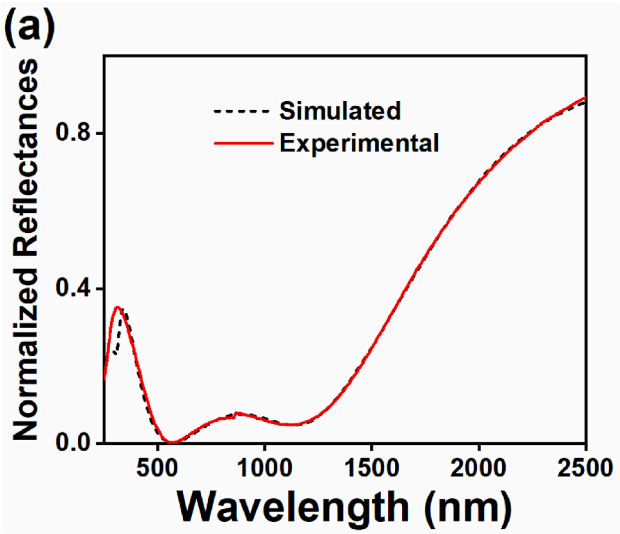

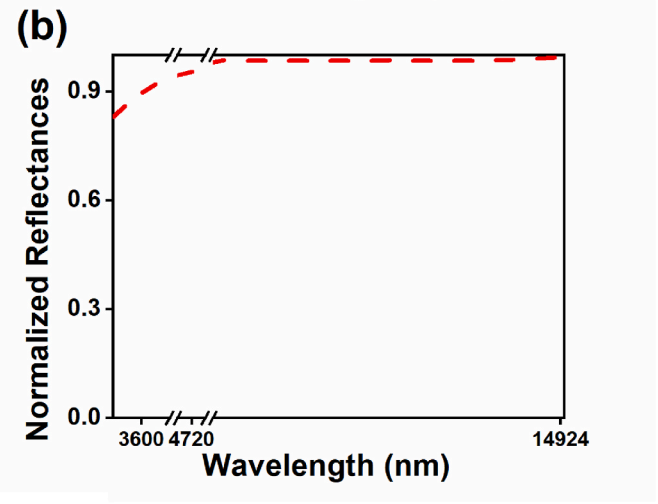

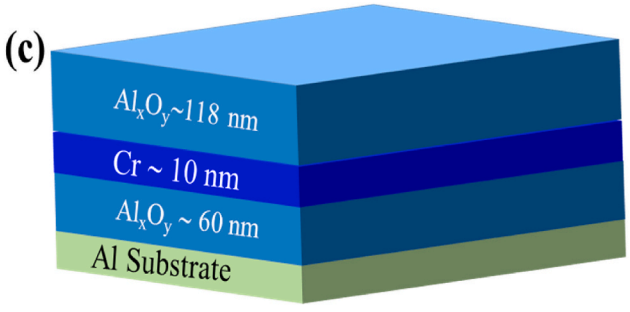

Fig. 9. Experimental and simulated spectral reflectance curve for the optimized $Al_xO_y/Cr/Al_yO_x$ multilayer coating on Al substrate (a,b) and Schematic diagram of the deposited multilayer stack (c).

Funding

This work was financially supported by the Ministry of Education, Science and Technology of Tanzania (MoEST), The University of Dar es Salaam, Materials Science and Solar Energy for Eastern and Southern Africa (MSSEESA), University of Pretoria, SARCHI UID No.115463 and the International Science Programme (ISP) - Uppsala University.

Declaration of competing interest

The authors declare that they have no known competing financial interests or personal relationships that could have appeared to influence the work reported in this paper.

Data availability

Data will be made available on request.

Acknowledgements

J Tibaijuka acknowledges the scholarship support from the Ministry of Education, Science and Technology of Tanzania (MoEST). The University of Dar es Salaam, the University of Pretoria, the Materials Science and Solar Energy Network for Eastern and Southern Africa (MSSEESA), SARCHI UID No.115463, and the International Science Programme (ISP) - Uppsala University, Sweden are also acknowledged by the authors for providing research facilities and materials support, as well as logistical and financial support during J.T. lab's stay at the University of Pretoria.

References

[1] N. Khoza, Z.Y. Nuru, J. Sackey, L. Kotsedi, N. Matinise, C. Ndlangamandla, M. Maaza, Structural and optical properties of $ZrO_x/Zr/ZrO_x/Al_xO_y$ multilayered coatings as selective solar absorbers, J. Alloys Compd. 773 (2019) 975–979, https://doi.org/10.1016/j.jallcom.2018.09.329.

[2] A. Al-Rjoub, L. Rebouta, P. Costa, N.P. Barradas, E. Alves, P.J. Ferreira, K. Abderrafi, A. Matilainen, K. Pischow, A design of selective solar absorber for high temperature applications, Sol. Energy 172 (2018) 177–183, https://doi.org/10.1016/j.solener.2018.04.052.

[3] Z.Y. Nuru, C.J. Arendse, T.F.G. Muller, M. Maaza, Structural and optical properties of $Al_xO_y/Pt/Al_xO_y$ multilayer absorber, Mater. Sci. Eng. B 177 (2012) 1194–1199, https://doi.org/10.1016/j.mseb.2012.05.028.

[4] J. Feng, S. Zhang, Y. Lu, H. Yu, L. Kang, X. Wang, Z. Liu, H. Ding, Y. Tian, J. Ouyang, The spectral selective absorbing characteristics and thermal stability of SS/TiAlN/TiAlSiN/Si_3N_4 tandem absorber prepared by magnetron sputtering, Sol. Energy 111 (2015) 350–356, https://doi.org/10.1016/j.solener.2014.11.005.

[5] V. Pelenovich, H. Liu, X. Zeng, Y. Liu, K. Liu, B. Yang, Graded solar selective absorbers deposited by non-equilibrium RF magnetron sputtering, Sol. Energy Mater. Sol. Cells 230 (2021), 111188, https://doi.org/10.1016/j.solmat.2021.111188.

[6] Y. Wu, E.T. Hu, Q.Y. Cai, J. Wang, Z.Y. Wang, H.T. Tu, K.H. Yu, L.Y. Chen, W. Wei, Enhanced thermal stability of the metal/dielectric multilayer solar selective absorber by an atomic-layer-deposited Al_2O_3 barrier layer, Appl. Surf. Sci. 541 (2021), 148678, https://doi.org/10.1016/j.apsusc.2020.148678.

[7] X. Ling, R. Wang, W. Wang, W. Nie, Microstructure and optical properties of W/W-W_xN/WO_x multilayer metal-dielectric solar selective absorbing coating, Surf. Interface Anal. 54 (2022) 1121–1129, https://doi.org/10.1002/sia.7136.

[8] J. Liu, Z.Q. Sun, H. Wang, Design and characterization of solar absorbing multilayer stack based on Al/Cr-NO/SiO_2 layers, Sol. Energy Mater. Sol. Cells 188 (2018) 18–26, https://doi.org/10.1016/j.solmat.2018.06.013.

[9] C.G. Granqvist, Solar energy materials, Adv. Mater. 15 (2003) 1789–1803, https://doi.org/10.1002/adma.200300378.

[10] T.K. Tsai, S.J. Hsueh, J.S. Fang, Optical properties of $Al_xO_y/Ni/Al_xO_y$ multilayered absorber coatings prepared by reactive DC magnetron sputtering, J. Electron. Mater. 43 (2013) 229–235, https://doi.org/10.1007/s11664-011-1746-2.

[11] E. Hu, X. Liu, Y. Yaob, K. Zang, Z. Tub, A. Jiang, K. Yu, J. Zheng, W. Wei, Y. Zheng, R. Zhang, S. Wang, H. Zhao, O. Yoshie, Y. Leed, C. Wange, D.W. Lynche, J. Guof, L. Chen, Multilayered metal-dielectric film structure for highly efficient solar selective absorption, Mater. Res. Express 5 (2018) 66428–66438, https://doi.org/10.1088/2053-1591/aacdb3.

[12] A. Dan, H.C. Barshilia, K. Chattopadhyay, B. Basu, Solar energy absorption mediated by surface plasma polaritons in spectrally selective dielectric-metal-dielectric coatings: a critical review, Renew. Sustain. Energy Rev. 79 (2017) 1050–1077, https://doi.org/10.1016/j.rser.2017.05.062.

[13] Q. Xiao, Analysis of High-Temperature Solar Selective Coating, PhD Thesis, Duke University, 2018.

[14] H.C. Barshilia, N. Selvakumar, K.S. Rajam, A. Biswas, Structure and optical properties of pulsed sputter deposited $Cr_xO_y/Cr/Cr_2O_3$ solar selective coatings, J. Appl. Phys. 103 (2008) 23507–23518, https://doi.org/10.1016/j.jallcom.2011.08.052.

[15] N. Selvakumar, H.C. Barshilia, K.S. Rajam, A. Biswas, Structure, optical properties and thermal stability of pulsed sputter deposited high temperature $HfO_x/Mo/HfO_2$ solar selective absorbers, Sol. Energy Mater. Sol. Cells 94 (2010) 1412–1420, https://doi.org/10.1016/j.solmat.2010.04.073.

[16] Z.Y. Nuru, M. Msimanga, T.F.G. Muller, C.J. Arendse, C. Mtshali, M. Maaza Microstructural, Optical properties and thermal stability of MgO/Zr/MgO multilayered selective solar absorber coatings, Sol. Energy 111 (2015) 357–363, https://doi.org/10.1016/j.solener.2014.11.009.

[17] Z.Y. Nuru, D. Perez, K. Kaviyarasu, A. Vantomme, M. Maaza, Annealing effect on the optical properties and inter-diffusion of MgO/Zr/MgO multilayered selective solar absorber coatings, Sol. Energy 120 (2015) 123–130, https://doi.org/10.1016/j.solener.2015.07.022.

[18] H.C. Barshilia, N. Selvakumar, G. Vignesh, K.S. Rajam, A. Biswas, Optical properties and thermal stability of pulsed-sputter-deposited $Al_xO_y/Al/Al_xO_y$ multilayer absorber coatings, Sol. Energy Mater. Sol. Cells 93 (2009) 315–323, https://doi.org/10.1016/j.solmat.2008.11.005.

[19] J.A. Thornton, A.S. Penfold, J.L. Lamb, Sputter-deposited $Al_2O_3/Mo/Al_2O_3$ selective absorber coatings, Thin Solid Films 72 (1980) 101–110, https://doi.org/10.1016/0040-6090(80)90563-5.

[20] A.B. Khelifa, S. Khamlich, Z.Y. Nuru, L. Kotsedi, A. Mebrahtu, M. Balgouthi, A. A. Guizani, W. Dimassi, M. Maaza, Growth and characterization of spectrally selective $Cr_2O_3/Cr/Cr_2O_3$ multilayered solar absorber by e-beam evaporation, J. Alloys Compd. 734 (2018) 204–209, https://doi.org/10.1016/j.jallcom.2017.11.036.

[21] A.B. Khelifa, A. Soum-Glaude, S. Khamlich, H. Glénat, M. Balghouthi, A.A. Guizani, M. Maaza, W. Dimassi, Optical simulation, characterization and thermal stability of $Cr_2O_3/Cr/Cr_2O_3$ multilayer solar selective absorber coatings, J. Alloys Compd. 783 (2019) 533–544, https://doi.org/10.1016/j.jallcom.2018.12.286.

[22] N. Khoza, Z.Y. Nuru, J. Sackey, L. Kotsedi, N. Matinise, C. Ndlangamandla, M. Maaza, Structural and optical properties of $ZrO_x/Zr/ZrO_x/Al_xO_y$ multilayered coatings as selective solar absorbers, J. Alloys Compd. 773 (2019) 975–979, https://doi.org/10.1016/j.jallcom.2018.09.329.

[23] R. Subasri, K.S. Raju, D.S. Reddy, N.Y. Hebalkar, G. Padmanabham, Sol–gel derived solar selective coatings on SS 321 substrates for solar thermal applications, Thin Solid Films 598 (2016) 46–53, https://doi.org/10.1016/j.tsf.2015.12.002.

[24] Z.Y. Nuru, *Spectrally Selective $Al_xO_y/Pt/Al_xO_y$ Solar Absorber Coatings for High Temperature Solar-Thermal Applications*, PhD Thesis, University of Western Cape, 2014.

[25] M.M. Singh, G. Vijaya, M.S. Krupashankara, B.K. Sridhara, T.N. Shridhar, Deposition and characterization of aluminium thin film coatings using DC magnetron sputtering process, Mater. Today Proc. 5 (2018) 2696–2704, https://doi.org/10.1016/j.matpr.2018.01.050.

[26] P.N. Dyachenko, S. Molesky, A.Y. Petrov, M. Stormer, T. Krekeler, S. Lang, M. Ritter, Z. Jacob, M. Eich, Controlling thermal emission with refractory epsilonnear-zero metamaterials via topological transitions, Nat. Commun. 7 (2016), 11809, https://doi.org/10.1038/ncomms11809.

[27] H. Wang, H. Alshehri, H. Su, L. Wang, Design, fabrication and optical characterizations of large-area lithography-free ultrathin multilayer selective solar coatings with excellent thermal stability in air, Sol. Energy Mater. Sol. Cells 174 (2018) 445–452, https://doi.org/10.1016/j.solmat.2017.09.025.

[28] J.J. Tibaijuka, M.E. Samiji, M. Diale, N.R. Mlyuka, Effects of multilayer structure on the microstructure and optical properties of the DC sputtered chromium thin films for selective solar absorber applications, Tanzan. J. Sci. 48 (3) (2022) 660–667, https://doi.org/10.4314/tjs.v48i3.13.

[29] J.J. Tibaijuka, M.E. Samiji, N.R. Mlyuka, Optimization of zinc to tin ratio in a sol gel precursor solution on the growth and properties of annealed CZTS thin films, Tanzan. J. Sci. 44 (4) (2018) 36–50.

[30] W. Theiss, SCOUT Optical Spectrum Simulation, W. Theiss Hard and Software, Achen, 2002.

[31] E.R. Ollotu, N.R. Mlyuka, M.E. Samiji, Effects of rapid thermal annealing on the properties of room-temperature oxygenated DC sputtered zinc thin films for CZTS solar cells application, Tanzan. J. Sci. 47 (2021) 637–647, https://doi.org/10.4314/tjs.v47i2.

[32] K.L. Choy, Chemical vapour deposition of coatings, Prog. Mater. Sci. 48 (2003) 57–170, https://doi.org/10.1016/S0079-6425(01)00009-3.

[33] Z.Y. Nuru, C.J. Arendse, R. Nemutudi, O. Nemraoui, M. Maaza, Pt–Al_2O_3 nanocoatings for high temperature concentrated solar thermal power applications, Phys. B Condens. Matter 407 (2012) 1634–1637, https://doi.org/10.1016/j.physb.2011.09.104.

[34] J.J. Tibaijuka, J.S. Nyarige, M. Diale, N.R. Mlyuka, M.E. Samiji, The effects of thermal treatment under argon–oxygen ambient on the microstructure and optical properties of DC sputtered Cr thin films for selective solar absorbers applications, J. Mater. Sci. Mater. Electron. 34 (2023) 173.

[35] A. Karoro, Z.Y. Nuru, L. Kotsedi, Kh Bouziane, B.M. Mothudi, M. Maaza, Laser nanostructured Co nanocylinders-Al_2O_3 cermets for enhanced and flexible solar selective absorbers applications, Appl. Surf. Sci. 347 (2015) 679–684, https://doi.org/10.1016/j.apsusc.2015.04.098.

[36] C. Sella, M. Maaza, B. Pardo, F. Dunsteter, J.C. Martin, M.C. Sainte Catherine, A. Kaba, Structural investigation of Pt–Al_2O_3